1997

# Surface Textural Analysis of Quartz Sand Grains from ODP Site 918 Off the Southeast Coast of Greenland Suggests Glaciation of Southern Greenland at 11 Ma

P. E. Helland
*University of Nebraska-Lincoln*

Mary Anne Holmes
*University of Nebraska-Lincoln*, mholmes2@unl.edu

Published in *Palaeogeography, Palaeoclimatology, Palaeoecology* (1997) 135: 109-121.  ISSN: 0031-0182. 

# Surface Textural Analysis of Quartz Sand Grains from ODP Site 918 Off the Southeast Coast of Greenland Suggests Glaciation of Southern Greenland at 11 Ma

P. E. Helland, M. A. Holmes*

Department of Geology, University of Nebraska-Lincoln, Lincoln, NE, USA
* Corresponding author: mholmes2@unl.edu

Received April 3, 1996; accepted January 24, 1997

Abstract
Shipboard analysis of the 1,183-m sedimentary section recovered at Site 918 in the Irminger Basin during Ocean Drilling Program Leg 152 revealed material of glacial origin (diamictons, ice-rafted debris (IRD) and dropstones) as deep as 543 m below sea floor (bsf). The sediment containing the deepest dropstone was biostratigraphically dated shipboard as approximately 7 Ma, pushing back the date for the onset of glaciation on southern Greenland by 5 Ma. Thin layers of fine sand were found as much as 60 m deeper in the core, raising the possibility of an even earlier date for glaciation. To determine the sedimentary history of these deeper sand layers, the surface textures on quartz grains from eleven cores bracketing the interval of interest were analyzed by scanning electron microscope. The results suggest that the grains in the 60-m interval below the deepest dropstone have a glacial history. At that level, an 11-Ma Sr-isotope date was obtained from planktonic foraminifers. This late Miocene timing is supported biostratigraphically by both nanofossil and foraminifer assemblages, indicating a new minimum age for the onset of glaciation on southern Greenland and in the North Atlantic.

Keywords: Late Miocene; glaciomarine; ice rafting; quartz sand; surface textures; North Atlantic

## 1. Introduction

One of the objectives of Ocean Drilling Program (ODP) Leg 152 was to investigate the glacial history of southern Greenland recorded in the sediments on its southeastern continental margin. Prior to this investigation the earliest record of glaciation of southern Greenland came from shelf sediments dated as 2 Ma (Funder, 1989). However, evidence of earlier glaciation in the North Atlantic region has been found at other localities. Tillites on Iceland yielded a 3.1-Ma date (McDougall and Wensink, 1966). A marine core from the central coast of Norway contains icerafted debris (IRD) dated to 5.45 Ma (Jansen et aI., 1990). IRD, biostratigraphically dated to the late Miocene (7.4 to 9.5 Ma), was recovered from a Baffin Bay core (Head *et al.*, 1989). These older dates raised the possibility that the onset of southern Greenland's glaciation occurred earlier as well. This possibility was realized by the recovery of glacial sediments in the upper 543 m of a 1,183-m-thick sedimentary sequence from ODP Site 918 in the Irminger Basin, 110 km off the coast of Greenland (Figure 1). Dropstones ranging in size from granules to boulders, beds of diamicton up to 10 m thick and fine-grained IRD were found suspended in a dark-gray silt (Larsen *et al.*, 1994; Shipboard Scientific Party, 1994). The clasts in the silty matrix were derived from both continental and volcaniclastic sources (Shipboard Scientific Party, 1994). An age of 7 Ma was derived for the deepest dropstone, at 543 mbsf, from nanofossil biostratigraphy and

sedimentation rates (Larsen *et al.*, 1994). However, thin layers of fine sand occur at least 60 m further down the section (Figure 2). Both the deeper sand layers and the overlying part of the sequence that contains the dropstones, diamictons, and IRD are part of the same lithologic unit (Shipboard Scientific Party, 1994). The low level of calcium carbonate, characteristic of the upper 543 m, also continues down the section to 600 mbsf (Larsen *et al.*, 1994). Below 600 mbsf there is a rapid, down-section transition from lower to higher levels of calcium carbonate and from cool water to warm water species of nanofossils. Although no process has been specified for emplacement of the deeper sand layers in the silt, Larsen *et al.* (1994) suggest that the 60-m interval may correspond to a climatic cooling when there was an increase in clastic material being delivered to the basin. Alternatively, the sand layers in the interval may be the earliest IRD

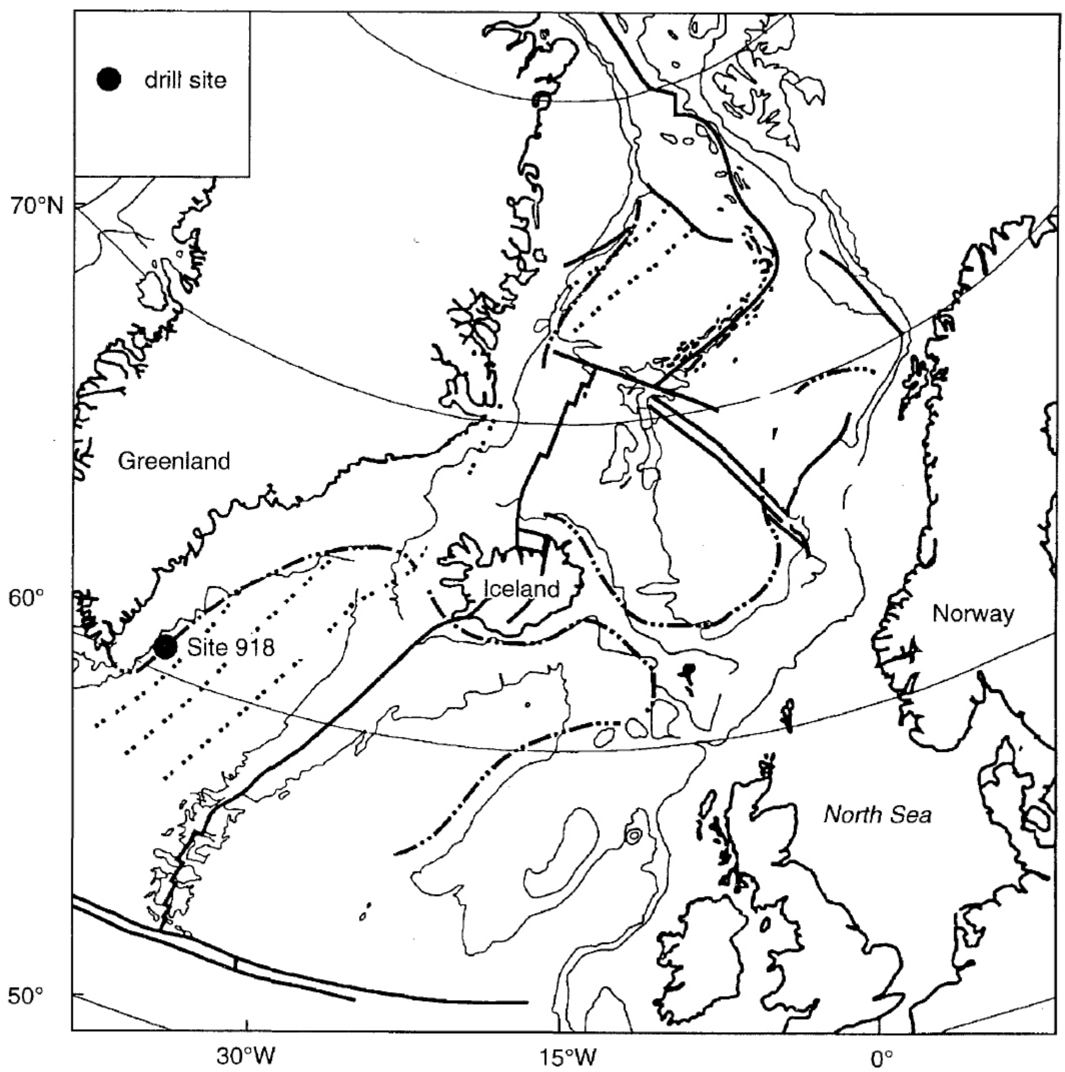


Fig. 1. Locality map showing Site 918 off the southeastern coast of Greenland.

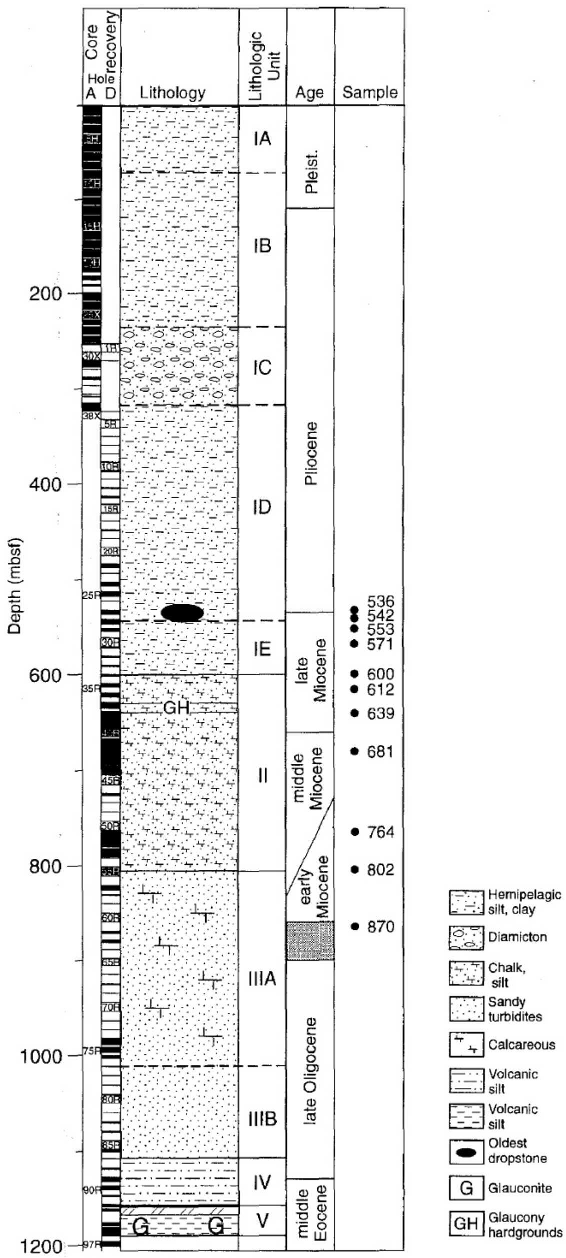


Fig. 2. Core recovery, lithology, lithologic unit and age of sediment recovered at Site 918, with location of samples analyzed for this study. Lithologic unit I, divided into 5 subunits based on abundance of glacial dropstones, comprises noncalcareous, hemipelagic mud. Lithologic unit II comprises interbedded volcaniclastic silt and nannofossil chalk interbeds. Lithologic units IV and V comprise volcaniclastic silt, the latter bearing abundant glauconite.

produced by glaciation of southern Greenland. If the deeper sand layers are also IRD, then glaciation of Greenland began earlier than 7 Ma. In this paper we discuss the sedimentary history, revealed by scanning electron microscope (SEM) surface textural analysis, of the quartz sand grains from eleven cores that include and bracket the 60-m interval of interest.

## 2. Methods

The cores selected for analysis are listed in Table 1 along with depth below sea floor of each core sample, a lithologic description of the sample locations, and the size of the largest grain analyzed. The sand grains used for the SEM analysis were those captured by the 63-μm sieve when the sediment from each core was prepared for clay analysis. The grains ranged up to 600 urn in diameter but most of the grains analyzed were between 200 and 400 μm. The samples were cleaned in boiling HCI and prepared for analysis following standard methods for this technique (Krinsley and Doornkamp, 1973; Bull, 1986). After this initial preparation, the grains were found heavily coated with clay and required an additional 24-h bath in sodium hexametaphosphate (Calgon) solution to clear the grain surfaces for viewing. Samples were assigned random numbers to conceal their stratigraphic order during viewing and analysis. Thirty to forty quartz grains were randomly selected from each sample and mounted on aluminum specimen stubs. These were coated with carbon and analyzed by energy-dispersive X-ray (EDX) to assure that the grains were quartz. Then the grains were coated with gold and viewed in the JOEL JSM-T330 SEM at 15 kV. Each grain in each sample was evaluated for the presence or absence of twenty-seven surface textures (Table 2) and the results compiled into a surface texture-percent frequency graph for each sample. To assess the sedimentary history of the samples, the grain morphology and surface textures that typify each sample are compared to those reported for quartz grains from sediments including IRD, reworked glaciomarine, turbidite, and beach sand.

Table 1
Data for sampled cores from ODP Hole 918D

| Sample No. | OPD designation: Leg-Core-Section, interval (cm) | Depth (mbsf) | Lithologic description of sample location | Largest grain size (μm) |
|---|---|---|---|---|
| 1 | 152-27R-03, 120–122 | 536 | siltstone with IRD | 400 |
| 2 | 152-28R-01, 50–52 | 542 | quartz silt with feldspar and clay | 350 |
| 3 | 152-29R-02, 38–40 | 553 | volcanic silt with clay and silt | 400 |
| 4 | 152-31R-01, 50–52 | 571 | volcanic silt | 200 |
| 5 | 152-34R-01, 68–70 | 600 | volcanic silt with quartz and micritc chalk | 400 |
| 6 | 152-35R-03, 30–32 | 612 | quartz silt and calcareous siltstone with sand | 350 |
| 7 | 152-38R-02, 22–24 | 639 | volcanic siltstone with nannofossils | 400 |
| 8 | 152-42R-04, 54–56 | 681 | nannofossil chalk with ash and volcanic silt | 400 |
| 9 | 152-51R-02, 0–5 | 764 | silty nannofossil chalk and volcanic silt | 300 |
| 10 | 152-55R-01, 79–81 | 802 | nannofossil chalk and glauconitic silt | 550 |
| 11 | 152-62R-01, 116–118 | 870 | siltstone with nannofossils and turbitic sand | 600 |

Lithologic description from Shipboard Scientific Party (1994).

Table 2
Surface textures used in analysis

| # Morphological | # Mechanical | # Chemical |
|---|---|---|
| 1. Angular outline | 6. Small conchoidal fracture | 21. Solution pits |
| 2. Rounded outline | 7. Large conchoidal fracture | 22. Chemical V-shaped pits |
| 3. Low relief | 8. Straight steps | 23. Adhering particles |
| 4. Medium relief | 9. Arcuate steps | 24. Limited silica precipitation |
| 5. High relief | 10. Imbricated blocks | |
| | 11. Large breakage blocks | 25. Extensive silica precipitation |
| | 12. Fractured plates | |
| | 13. Striations | 26. Oriented soln./precip. |
| | 14. Edge abrasion | 27. Euhedral crystal overgrowths |
| | 15. Mechanical V-shaped pits | |
| | 16. Straight grooves | |
| | 17. Curved grooves | |
| | 18. Meandering ridges | |
| | 19. Irregular depressions | |
| | 20. Upturned plates | |

List of textures derived from the work of others: Krinsley and Donahue (1968), Margolis and Kennett (1971), Higgs (1979), and Bull (1986).

## 3. Results

### 3.1. Samples 1 and 2

The samples from the cores that contain dropstones, at 536 and 542 m below sea floor (bsf) (Figure 2), are composed of predominantly angular to subangular grains with medium relief (Figures 3 and 4A-D). The grains bear numerous mechanical breakage textures (Table 2, textures 6-12) that include conchoidal fracture, straight and arcuate steps, large breakage blocks, and fractured plates. Of the mechanical textures previously reported to be associated with sediment transport (Margolis and Kennett, 1971; Krinsley and Doornkamp, 1973; Bull, 1986), only edge abrasion (textures 13-20, Figure 4E) occurs with sufficient frequency in the samples to be notable. The predominant forms of chemical alteration are solution pits (texture 21, Figure 4E) and

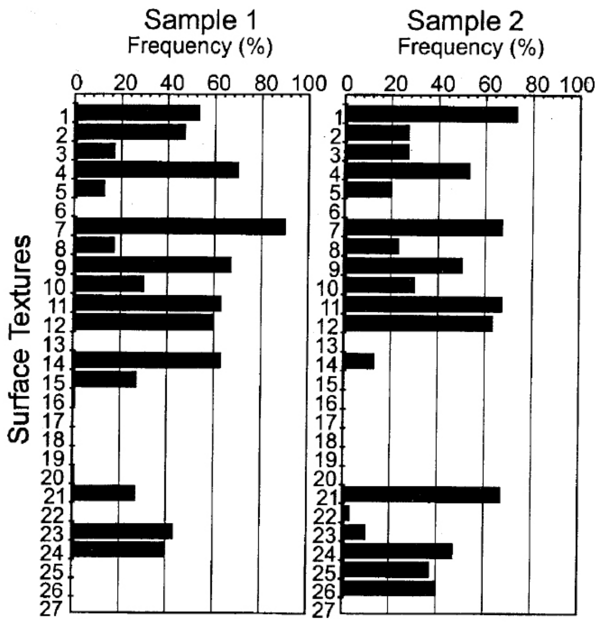


Fig. 3. Frequency of surface textures 1–27 (Table 2) in samples 1 and 2, from the interval containing the dropstones, at 536 and 542 mbsf.

amorphous silica precipitation (texture 24, Figures 4D and F).

### 3.2. Samples 3-5

The samples taken from the 60-m interval below the deepest dropstone (Figure 2) are angular to subangular with medium to high relief (Figure 5 and Figures 6A, C). These grains also possess numerous mechanical breakage textures that occur with a slightly higher frequency than those in the overlying samples (Figure 3). In addition to edge abrasion, parallel striations, and straight grooves (textures 13 and 16, Table 2) are found in sample 5 (Figure 6B and D). Chemical alteration in these samples is comparable to that in sample 2.

### 3.3. Samples 6-9

Samples from 600 to 764 mbsf (Figure 2) have predominantly subrounded grains with medium relief (Figures 7 and 8A, B). As with the previous samples, these grains show a moderate to high frequency of mechanical breakage textures. Although these grains have few textures associated with sediment transport, there is a downcore increase in the frequency of edge abrasion (texture 14) and mechanical V-shaped pits (texture 15). Both the number and frequency of chemical textures are greater than in the previous samples and include crystal overgrowths (texture 27) and abundant chemical V-shaped pits (texture 22) (Figures 8C and D).

### 3.4. Samples 10 and 11

The quartz grains from the deepest samples, 802 and 870 mbsf (Figure 2), are rounded to well-rounded with medium to low relief (Figures 9 and 10, A and B). Unlike the grains in the previous samples, the grains in these samples exhibit abundant mechanical V-shaped pits and irregular pits which are associated with high-energy subaqueous transport (Figures 10C and D).

## 4. Discussion

### 4.1. Evidence of a glacial history in samples 1-5

There is a strong similarity in the surface texture frequencies among the samples taken from the five highest cores (536-600 mbsf). Most of the grains in samples 1 and 2, which come from the cores containing dropstones (Figure 3) and in samples 3-5, which come from the 60 m deeper interval (Figure 5), have surface textures associated with glacially influenced grains (Margolis and Kennett, 1971; Krinsley and Doornkamp, 1973; Bull, 1986). A high frequency of angular to subangular grains is reported for englacia1 and supraglacial samples from modern glaciers (Whalley and Krinsley, 1974) and glaciomarine grains found in deep-sea cores (Blank and Margolis, 1975; Mazzulo and Anderson, 1987). Samples 1-5 also show the wide range of breakage textures (textures 6-12, Table 2) occurring with the high frequencies reported for glacial samples (Margolis and Kennett, 1971; Krinsley and Doornkamp, 1973; Bull, 1986). Since these textures may be produced by other processes (Whalley and Krinsley, 1974; Krinsley, 1980), they are a

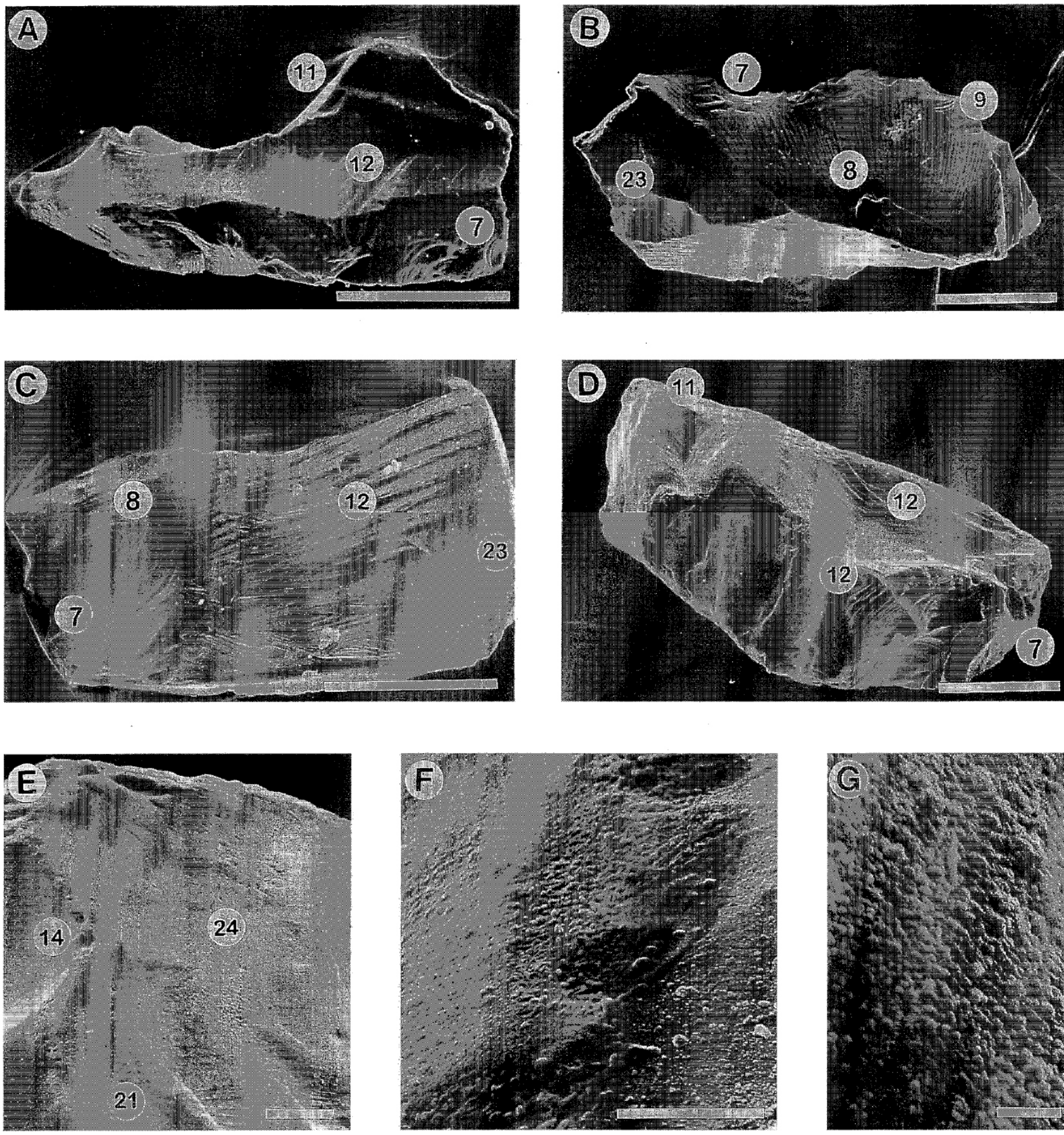


Fig. 4. SEM micrographs of grains from the samples 1 and 2, associated with dropstones (536–542 mbsf). (Texture numbers correspond to those used in Table 2.).

A–D. Angular to subangular grains with medium relief bearing numerous mechanical textures: conchoidal fracture (7) with straight steps (8), arcuate steps (9), large breakage blocks (11), and fractured plates (12). Also adhering particles (23) are apparent on the surfaces of grains in (A) and (C). *Scale bars* = 100 μm.

E. Edge abrasion (14) traces the boundary between two grain faces which are smoothed by amorphous silica precipitation (24). Areas of low elevation are affected by silica solution (21). *Scale bar* = 100 μm.

F. Grain surfaces coated by a combination of silica spherules and amorphous silica. *Scale bar* = 5 μm.

G. Silica spherules at higher magnification. *Scale bar* = 1 μm.

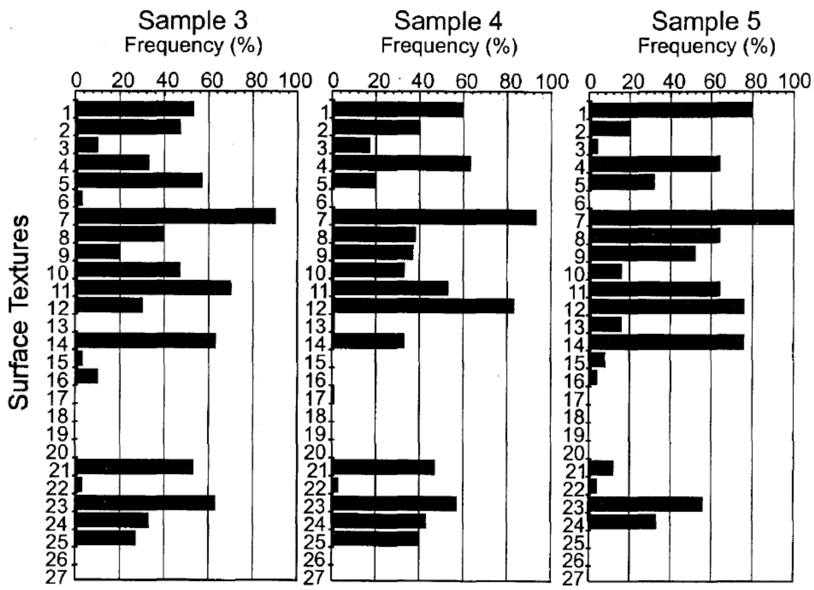


Fig. 5. Frequency of surface textures 1–27 in samples 3–5, from the 60-m interval below the dropstones, between 553 and 600 mbsf.

necessary, but not sufficient, indicator of a glacial history. In fact, the number and frequency of breakage textures do not discriminate well among the study samples. Breakage textures are present with the highest frequency in the upper five samples, but grains in all of the study samples bear many of these textures. Edge abrasion, a mechanical texture that is reported by many workers to be associated with glacial transport (Whalley, 1978; Whalley and Langway, 1980, Figure 3; Dowdeswell, 1982, Figure 5; Sharp and Gomez, 1986; Mahaney *et al.*, 1988), is present in all five samples. In addition, grains from sample 5, from 600 mbsf, also bear striations and straight grooves (Figures 5B and D). Striations appear to be strongly indicative of glacial processing (Krinsley and Doornkamp, 1973; Bull, 1986). Adhering particles, present in these samples on greater than 50% of the grains, is also characteristic for glacially influenced grains (Krinsley and Doornkamp, 1973; Whalley and Krinsley, 1974; Mazzullo and Ritter, 1991). There is sufficient similarity (1) among the five samples and (2) with reported glacially associated morphology and textures, to infer that all are IRD, transported to the Irminger Basin by glacial ice. That the two highest samples come from cores that contain dropstones adds strength to this inference. The glacial signature is most strongly expressed in sample 5, from the base of the 60-m interval below the deepest dropstone at 600 mbsf.

Further indications that glaciation of southern Greenland may have been ongoing when the sediments in the 60-m interval of interest were deposited come from analysis of microfossils within the sedimentary sequence. Wei (1997) observes that warm-water nanofossil taxa, which were present downcore, disappear at 650 mbsf and remain absent in the overlying cores. This transition, biostratigraphically dated to approximately 12 Ma, was interpreted as signaling a precipitous cooling of the sea off southeastern Greenland. Planktonic foraminifers also indicate that cool conditions with glacial events predominated in the upper Miocene interval of the cores, approximately 515-620 mbsf (Spezzaferri, 1997). Microfossil analysis of another deep-sea core reveals a cooling period between 11.4 and 12.9 Ma (Woodruff and Savin, 1991). This is based on peaks in $\delta^{18}O$ for the benthic foraminifer genus, *Cibicidoides*, from the DSDP Atlantic Ocean Site 563 at 33°N latitude.

Although no date has been obtained for the base of the 60-m interval of interest, at 600 mbsf

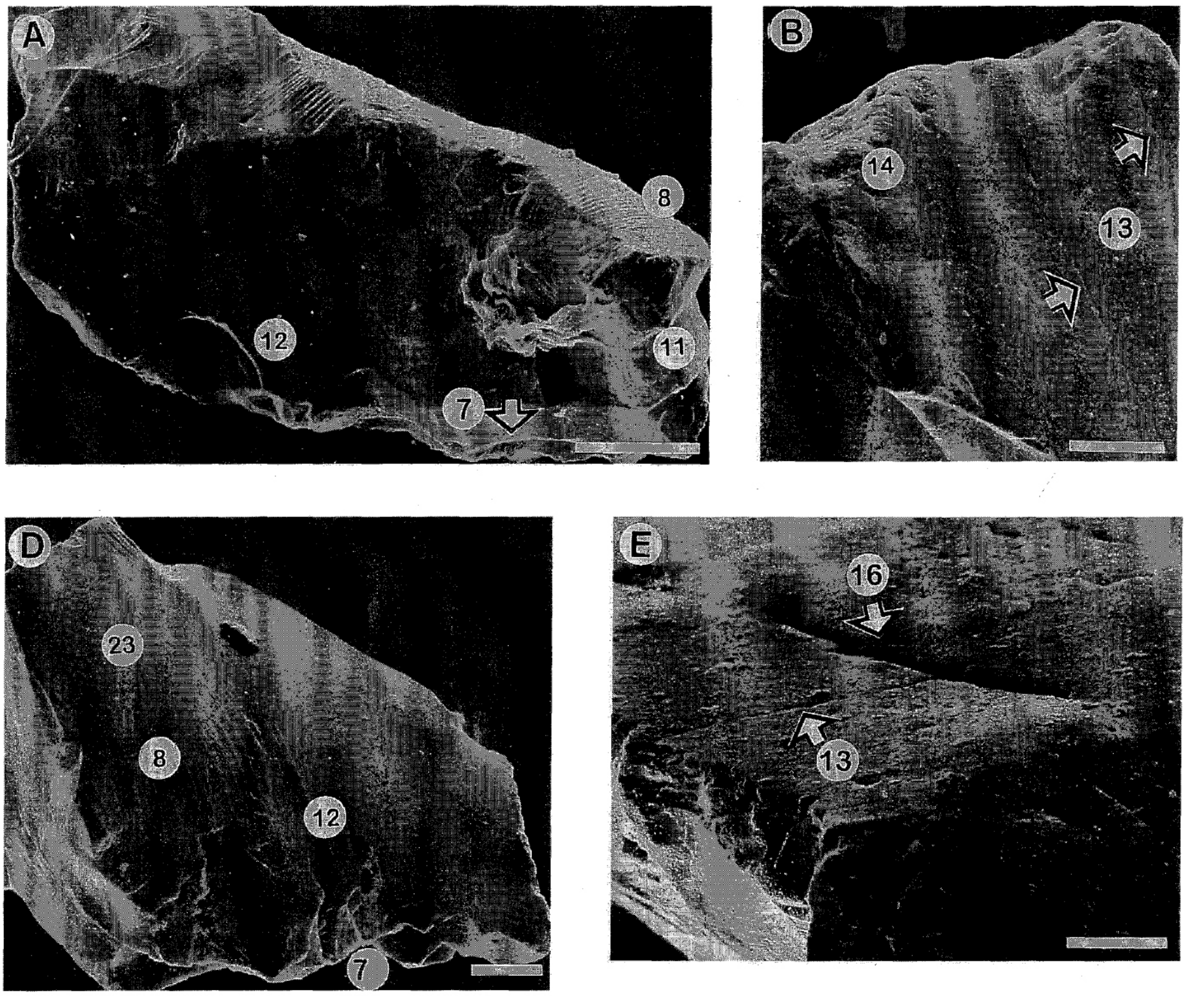


Fig. 6. SEM micrographs of grains from samples 3–5 (553–600 mbsf).

A and C. Angular to subangular grains with medium relief showing conchoidal fracture (7), straight steps (8), large breakage blocks (11), and fractured plates (12). Adhering particles (23) can be seen on grains. *Scale bar* for (A) = 100 μm, for (C) = 10 μm.

B. Edge abrasion (14) is well developed on this grain. Note parallel striations (13) on the spherule coated grain face. *Scale bar* = 50 μm.

D. In addition to striations this grain has deep straight grooves (16). Note silica spherules detectable along bright abraded edge. *Scale bar* = 50 μm.

(Figure 2), Israelson and Spezzaferri (1997) bracketed this level with Sr-isotope dates of 11.0 ± 0.8 Ma at 591 mbsf and 10.8 ± 0.8 at 621 mbsf. Both dates were based on Sr isotopes from planktonic foraminifers. Specimens showing evidence of reworking or diagenesis were excluded from the analysis. The data were normalized to the NBS987 value of $^{87}Sr/^{86}Sr$ = 0.710255. The ages were calculated using the Oslick *et al.* (1994) equation for 9.9-15.2 Ma based on the geomagnetic polarity time scale of Cande and Kent (1992).

The paleontological date closest to 600 mbsf is reported by Wei (1997) who used the last occurrence of the nanofossil, *Coccolithus miopelagicus*, to infer an age of 11.5 Ma at 632 mbsf. These dates point to 11 Ma as an acceptable approx-

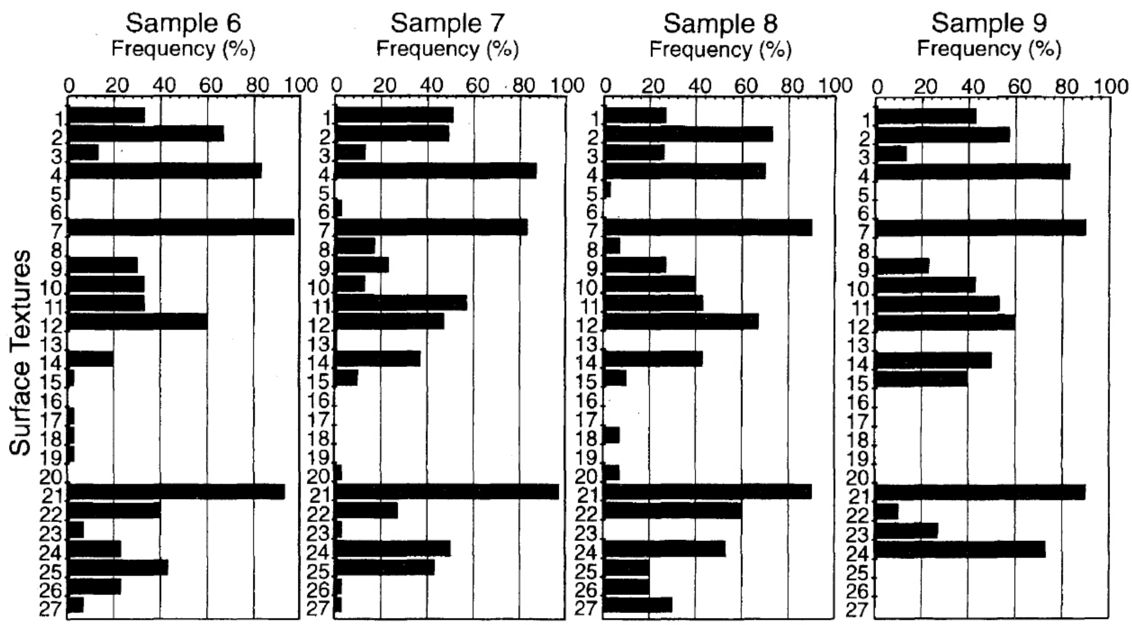


Fig. 7. Frequency of surface textures 1–27 in samples 6–9, between 612 and 764 mbsf.

imation for the age of the base of the 60-m interval of interest and the onset of glaciation of southern Greenland.

4.2. Unclear sedimentary history of samples 6-9

Surface textural analysis of samples 6-9 (Figure 7), from 612 to 764 mbsf, does not give a clear indication of their sedimentary history. The roundness of the grains, lower frequency of mechanical breakage textures, high frequency of silica solution and precipitation textures, as well as chemical V-shaped pits, are characteristics that could be produced by subaerial weathering (Krinsley and Doornkamp, 1973; Bull, 1986) or subaqueous dissolution by sea water (Margolis and Krinsley, 1974). The euhedral crystal overgrowths present in samples 6-8 are reported on subaerially weathered grains (Margolis and Krinsley, 1974) and on grains that have undergone diagenesis (Bull, 1986). While the frequency of edge abrasion indicates erosion or transport where there is grinding of the surface, the low frequency of mechanical V-shaped pits in these three samples suggests limited subaqueous transport, not consistent with beach or turbiditic processes. Only sample 9 in the 612-764-mbsf interval has a high enough frequency of mechanical V-shaped pits to suggest that the grains may have undergone high-energy subaqueous transport. The descriptions of the cores do not aid in understanding the depositional history of the grains in these samples, as cores were moderately to strongly bioturbated (Shipboard Scientific Party, 1994).

4.3. Indications of subaqueous or turbiditic processes in samples 10 and 11

The sedimentary history of some of the grains in samples 10 and 11, from 802 and 870 mbsf, are more clearly indicated. These samples contain 70% and 63% rounded to well-rounded grains. In both samples the grains roughly divide into two groups:

(1) rounded grains of medium relief, showing large breakage blocks, relict mechanical breakage textures obscured by the heavy coating of amorphous silica, and scattered mechanical V-shaped pits on the ridges between the grain surfaces (Figure 10 A); and (2) well-rounded grains of low relief, with abundant mechanical V-shaped pits and irregular depressions contain-

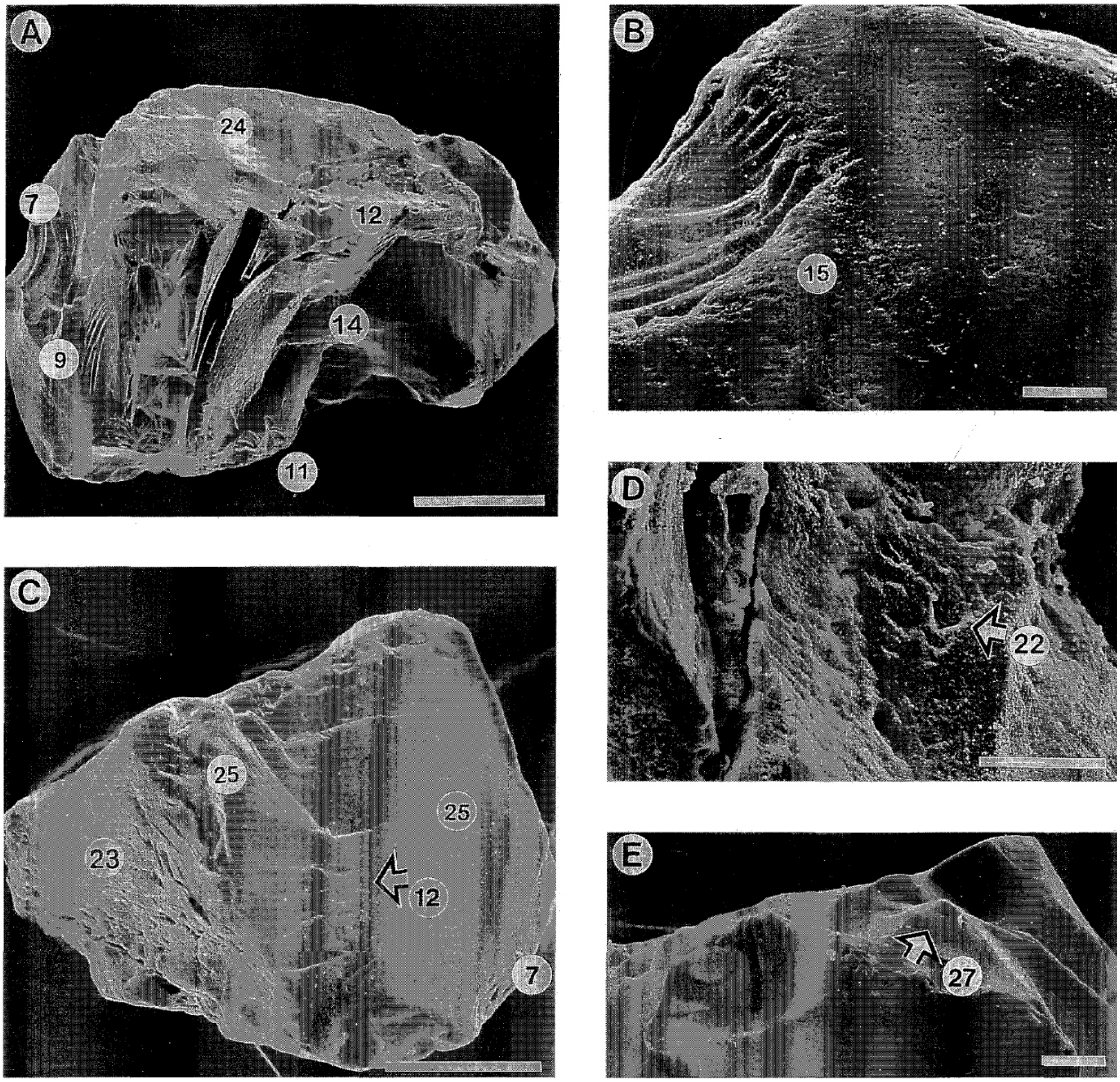


Fig. 8. SEM micrographs of grains from samples 6–9 (612–764 mbsf).

A. Grain from sample 7. Sub-rounded grain with medium relief bearing conchoidal fracture (7), arcuate steps (9) large breakage blocks (11), fractured plates (12), edge abrasion (14), and an amorphous silica coating (24). *Scale bar* = 100 μm.

B. Areas of high relief on the grain's surfaces have small mechanical V-shaped pits (15). *Scale bar* = 50 μm.

C. Grain from sample 9. Although conchoidal fracture (7) and fractured plates (12) can still be distinguished, amorphous silica (25) thickly coats the grain. Note area of silica solution (21). *Scale bar* = 100 μm.

D. Chemical V-shaped pits (22) occupy areas of low relief on grain. Silica spherules coat grains. *Scale bar* = 10 μm.

E. Note crystal overgrowths (27). *Scale bar* = 10 μm.

ing fresh mechanical breakage textures. These grains lack an amorphous silica indicates different histories for the two groups. coating (Figure 10 B). That the grains in the samples The thick coat of amorphous silica on the grains are composed of two distinguishable populations in the

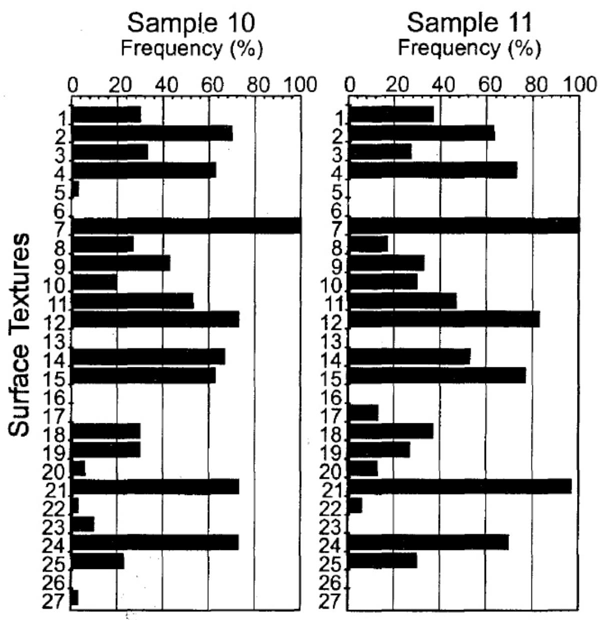


Fig. 9. Frequency of surface textures 1–27 in samples 10 and 11, between 802 and 870 mbsf.

first group suggests subaerial weathering (Krinsley and Doornkamp, 1973). The presence of the V-shaped pits in the coated surface indicates subsequent subaqueous transport with limited reworking, or transport by a relatively low-energy process so that grain to grain impact or sliding was minimal and the resultant V-shaped pits, limited (Goodale and Hampton, 1987). The low number of V-shaped pits per grain suggests a component of fluvial or low-energy beach transport for these grains (Bull, 1986).

In the second group, the extent of rounding and high density of V-shaped pits on the grains indicate more energetic subaqueous transport (Krinsley and Doornkamp, 1973; Bull, 1986; Goodale and Hampton, 1987). The occurrence of V-shaped pits of several different sizes suggests multiple episodes of reworking for this group. These grains correspond well to grains recovered from modern and ancient beach and turbidite deposits (Margolis and Kennett, 1971, plate 4, figs. A and B; Ingersoll, 1974, Figure 5; Bull, 1986; Krinsley and Marshall, 1987, Figures 3 and 4).

Shipboard description of the cores provides some clarification of the sedimentary history of the grains in the samples (Shipboard Scientific Party, 1994). Sedimentary textures and structures point to a turbiditic origin for sample 11. This sample came from lithologic subunit III A (806-1108 mbsf, Figure 2), which is composed of chalk interbedded with massive to weakly laminated silt and thin sand beds. Many of the contacts within the subunit are erosive and some sand beds show cross-lamination. Sample 11 comes from a fining upwards sand bed. Sample 10 came from a core that is strongly bioturbated, confounding an understanding of the sample's depositional history.

## 5. Conclusions

Surface textural analysis of the quartz sand grains from eleven cores in the 536-879-mbsf interval of the sedimentary sequence recovered at Site 918 suggests that grains down to the base of the 60-m interval below the deepest dropstone, at 600 mbsf, are ice-rafted debris. Paleontological information indicates that cool climatic conditions with glacial events predominated for the 515-620-mbsf interval of the core. This supports the possibility that the grains in the sample from 600 mbsf have a glacial history. The paleontological and Sr-isotope dates bracketing the 600-mbsf level yield an approximate age of 11 Ma for the deepest IRD. This suggests a new minimum age for the beginning of ice formation in southern Greenland and in the North Atlantic. While analysis of grains from 612 to 764 mbsf does not give a clear indication of sedimentary history, grains from 802 and 870 mbsf bear the surface textures of subaqueous transport. The surface textures present on some of the grains from 802 and 870 mbsf correspond well to high-energy turbidite grains. Sedimentary structures observed in the core support this inference, indicating that they were deposited in the Irminger Basin by turbiditic processes.

## Acknowledgements

We wish to thank the people who helped in the data gathering. Todd Voiles of the Central Facility for Electron Microscopy, Center for Materials Research and Analysis, University of Nebraska,

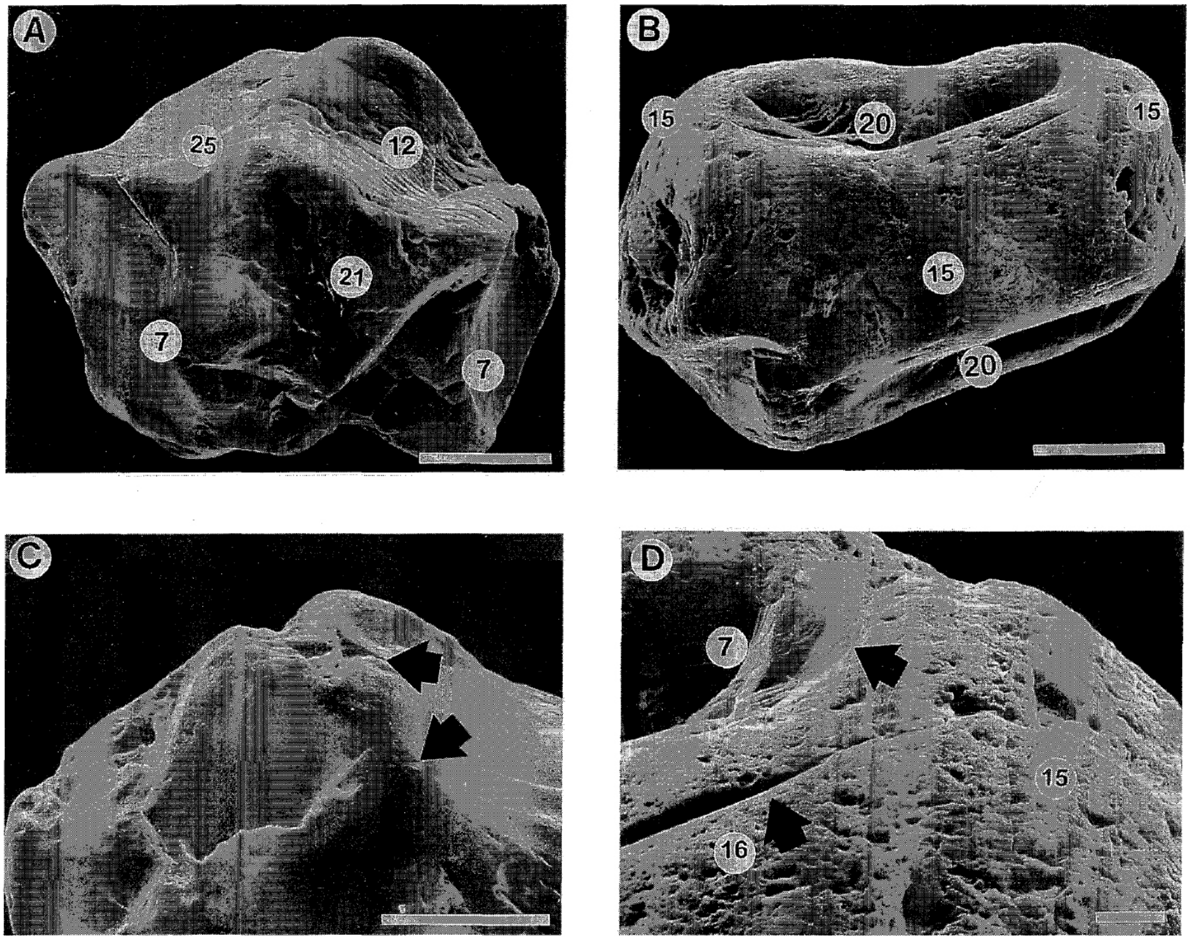


Fig. 10. SEM micrographs of grains form samples 10 and 11 (802–870 mbsf).

A. Rounded grain of medium relief. Here amorphous silica coating (25) obscure grains surface. Relict conchoidal fracture (7) and fractured plated (12) can still be detected. Note area of silica solution (21). *Scale bar* = 100 μm.

B. Well-rounded grain with numerous mechanical V-shaped pits (15) and irregular depressions (20). *Scale bar* = 100 μm.

C. Small mechanical V-shaped pits along ridge between grain faces smoothed by amorphous silica (*lower arrow*). Note very large mechanical V-shaped pits (*upper arrow*). *Scale bar* = 50 μm.

D. (Area from grain B.) At high magnification the surface of the grain shows different size populations of mechanical V-shaped pits (15) and straight grooves (16). Note the conchoidal breakage (7) in the irregular depression. *Scale bar* = 10 μm.

provided the EDX analysis of the sand grains. Debra Beck, Aradhna Srivastav, Diane Winter, and Dr. David K. Watkins gave technical assistance with the SEM analysis. Kraig Heiden and Justin Spence provided assistance with sample preparation. This work was funded by the Joint Oceanographic Institutions/U.S. Science Support Program.

References

Blank, R. G., Margolis, S. Y., 1975. Pliocene climatic and glacial history of Antarctica as revealed by southeast Indian Ocean deep-sea cores. *Bull. Geol. Soc. Am.* 86, 1,058-1,066.

Bull, P. A., 1986. Procedures in environmental reconstruction by SEM analysis. *In:* Sieveking, G. de G., Hart, M. B. (Eds.), The Scientific Study of Flint and Chert: *Proceedings of the Fourth International Flint Symposium,* Polytechnic, April 10-15, 1983: Cambridge. Cambridge University

Press, Cambridge, pp. 221-226.
Cande, S. C., Kent, D.V., 1992. A new geomagnetic polarity time scale for the Late Cretaceous and Cenozoic. *J. Geophys. Res.* 97, 13,917-13,951.
Dowdeswell, J. A., 1982. Scanning electron micrographs of quartz sand grains from cold environments examined using Fourier shape analysis. *J. Sediment. Petrol.* 40, 205-212.
Funder, S., 1989. Quaternary geology of the ice-free areas and adjacent shelves of Greenland. *In:* Fulton, R.J. (Ed.), *Quaternary Geology of Canada and Greenland.* Geol. Soc. Am., pp. 743-792.
Goodale, J. L., Hampton, M. A., 1987. An experimental and theoretical study of some quartz grain surface features. *In:* Marshall, J. R. (Ed.), *Clastic Particles: Scanning Electron Microscopy and Shape Analysis of Sedimentary and Volcanic Clasts.* Van Nostrand Reinhold, New York, NY, pp. 229-241.
Head, M. J., Norris, G., Mudie, P. J., 1989. Palynology and dinocyst stratigraphy of the Miocene in ODP Leg 105, Hole 645E, Baffin Bay. *In:* Srivastava, S. P., Arthur, M., Clement, B., *et al.* (Eds.), *Proceedings of the Ocean Drilling Program, Scientific Results,* Vol. 105. Ocean Drill. Prog., College Station, TX, pp. 423-550.
Higgs, R., 1979. Quartz-grain surface features of Mesozoic-Cenozoic sands from the Labrador and western Greenland continental margins. *J. Sediment. Petrol.* 49, 599-610.
Ingersoll, R. V., 1974. Surface textures of first cycle quartz sand grains. *J. Sediment. Petrol.* 44, 151-157.
Israelson, C., Spezzaferri, S., 1997. Strontium isotope stratigraphy from Ocean Drilling Program Sites 918 and 919. *In:* Larsen, H. C., Saunders, A. D., Clift, P. D., et al. (Eds.), *Proceedings of the Ocean Drilling Program, Scientific Results,* Vol. 152. Ocean Drill. Prog., College Station, TX (in press).
Jansen, E., Sjeholm, J., Bleil, D., Erichsen, J. A., 1990. Neogene and Pleistocene glaciations in the northern hemisphere and late Miocene-Pliocene global ice volume fluctuations: evidence from the Norwegian Sea. *In:* Bleil, O., Thiede, J. (Eds.), *Geological History of the Polar Oceans: Arctic Versus Antarctic.* Kluwer, Dordrecht, pp. 667-705.
Krinsley, D. H., 1980. Scanning electron microscope examination of quartz sand grain micro textures. *Kwart. Geol.* 24, 217-232.
Krinsley, D. H., Donahue, J., 1968. Environmental interpretation of sand grain surface textures by electron microscopy. *Bull. Geol. Soc. Am.* 79, 743-748.
Krinsley, D. H., Doornkamp, J. C., 1973. *Atlas of Quartz Sand Surface Textures.* Cambridge University Press, Cambridge, pp. 7-15.
Krinsley, D. H., Marshall, J. R., 1987. Sand grain textural analysis: an assessment. *In:* Marshall, J. R. (Ed.), *Clastic Particles: Scanning Electron Microscopy and Shape Analysis of Sedimentary and Volcanic Clasts.* Van Nostrand Reinhold, New York, NY, pp. 2-15.
Larsen, H. C., Saunders, A. D., Clift, P. D., Beget, J., Wei, W., Spezzaferri, S., 1994. Seven million years of glaciation in Greenland. *Science* 244, 952-955.
Mahaney, W. C., Vortisch, W., Julig, P., 1988. Relative differences between glacially crushed quartz transported by mountain and continental ice—some examples from North America and East Africa. *Am. J. Sci.* 288, 810-826.
Margolis, S. V., Kennett, J. P., 1971. Cenozoic paleoglacial history of Antarctica recorded in subantarctic deep-sea cores. *Am. J. Sci.* 271, 1-36.
Margolis, S. V., Krinsley, D. H., 1974. Processes of formation and environmental occurrence of microfeatures on detrital quartz grains. *Am. J. Sci.* 274, 449-464.
Mazzulo, J., Anderson, J. B., 1987. Glacial-marine sand grains from the Weddell and Ross Seas, Antarctic. *In:* Marshall, J.R. (Ed.), *Clastic Particles: Scanning Electron Microscopy and Shape Analysis of Sedimentary and Volcanic Clasts.* Van Nostrand Reinhold, New York, NY, pp. 314-327.
Mazzullo, J., Ritter, C; 1991. Influence of sediment source on the shape and surface textures of glacial quartz sand grains. *Geology* 19, 384-388.
McDougall, I., Wensink, H., 1966. Paleomagnetism and geochronology of the Pliocene-Pleistocene lavas in Iceland. *Earth Planet. Sci. Lett.* 1, 232.
Oslick, J. S., Miller, K. G., Feigenson, M. D., 1994. Oligocene-Miocene strontium isotopes: Stratigraphic revisions and correlation to an inferred glacioeustatic record. *Paleoceanography* 9, 427-433.
Sharp, M., Gomez, B., 1986. Processes of debris comminution in the glacial environment and implication for quartz sandgrain micromorphology. *Sediment. Geol.* 46, 33-47.
Shipboard Scientific Party, 1994. Site 918. *In:* Larsen, H. C., Saunders, A. D., Clift, P. D., *et al.* (Eds.), *Proceedings of the Ocean Drilling Program, Initial Reports,* Vol. 152. Ocean Drill. Prog., College Station, TX, pp. 177-256.
Spezzaferri, S., 1997. Plantonic foraminifer biostratigraphy and paleoenvironmental implications of Leg 152 sites (east Greenland margin). *In:* Larsen, H.C., Saunders, A. D., Clift, P.D., *et al.* (Eds.), *Proceedings of the Ocean Drilling Program, Scientific Results,* Vol. 152. Ocean Drill. Prog., College Station, TX (in press).
Wei, W., 1997. Calcareous nanofossils from the southeast Greenland margin: biostratigraphy and paleoceanography. *In:* Larsen, H. C., Saunders, A. D., Clift, P. D., *et al.* (Eds.), *Proceedings of the Ocean Drilling Program, Scientific Results,* Vol. 152. Ocean Drill. Prog., College Station, TX (in press).
Whalley, W. B., 1978. An SEM examination of quartz grains from sub-glacial and associated environments and some methods for their characterization. *Scanning Electron Miscrosc.* 1, 353-360.
Whalley, W. B., Krinsley, D. H., 1974. A scanning electron microscope study of surface textures of quartz grains from glacial environments. *Sedimentology* 21, 87-105.
Whalley, W.B., Langway, C. C., Jr., 1980. A scanning electron microscope examination of subglacial quartz grains from Camp Century core Greenland—a preliminary study. *J. Glaciol.* 25, 125-131.
Woodruff, F., Savin, S., 1991. Mid-Miocene isotope stratigraphy in the deep sea: high-resolution correlations, paleoclimatic cycles and sediment preservation. *Paleoceanography* 6, 755-806.